15.6 THE FORMATION AND INTENSIFICATION OF SUPERCRITICAL TORNADO-LIKE VORTICES—A LABORATORY STUDY

Christopher R. Church*, Karen A. Kosiba[#], J. David Cleland**, and Christopher P. Beer
Miami University, Oxford, Ohio
[#]Purdue University, West Lafayette, Indiana
**Rota Skipper Corporation, South Holland, Illinois

1. INTRODUCTION

Observations of tornadoes in the field and laboratory investigations of tornado-like end-wall vortices have both demonstrated the complexity of this fluid phenomenon. The structure of the core region in particular depends on a number of parameters, one being the swirl ratio (S), i.e the degree of swirl in the background flow (Davies-Jones, 1976), another being the degree of roughness of the underlying surface. These are
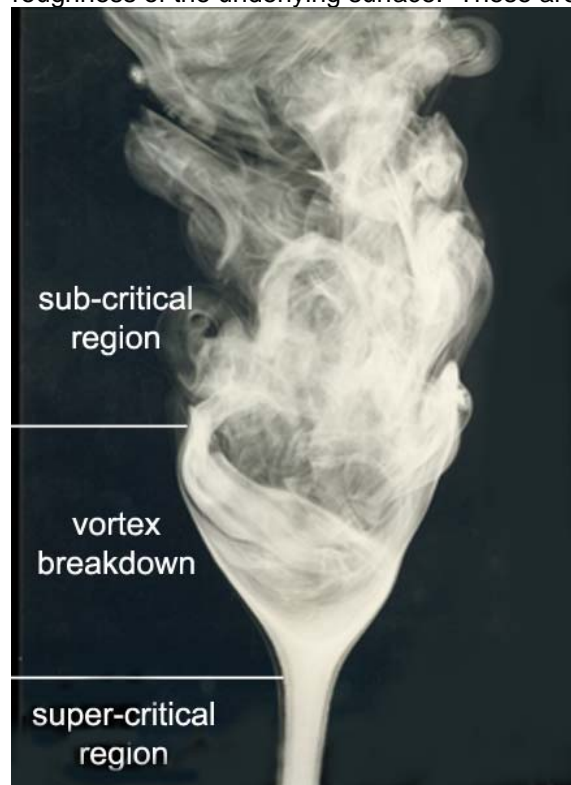
Figure 1. Photograph of laboratory vortex

_____

*Corresponding author address: Christopher R. Church, Miami University, Dept of Physics, Oxford OH 45056-1105; e-mail: churchcr@muohio.edu

principal factors in determining whether and at what level the core exhibits a 1-cell or a 2-cell structure, and the strength of the maximum winds. The 1-cell type, also referred to as a low-swirl, supercritical or (after Fujita) a "suction" vortex, is characterized by an intense upward spiraling flow throughout its relatively narrow core region, with an on-axis vertical velocity maximum. As the degree of swirl is increased the 1-cell vortex intensifies until it undergoes transition to a 2-cell type. The 2-cell type has a much broader core and lower velocities. Here the highest velocities are found in an annular region surrounding a turbulent center. Figure 1 shows a portion of a vortex that displays both 1-cell structure (lower part) and 2-cell structure (upper part). The bubble-like expansion in between is termed vortex breakdown (VBD), and for each incremental increase in swirl the VBD descends, until finally it reaches the surface and the vortex has become entirely a 2-cell structure.

With regard to the damage caused by tornadoes, we may attribute the most severe local damage (width~10m) to the 1-cell suction vortices, and the less devastating, more widespread damage (width~1000m) to the 2-cell type. The 2-cell type however, may also contain multiple suction vortices, resulting in general damage over a wide area, and within which there are spots of total devastation.

This paper summarizes our recent efforts to conduct a systematic laboratory investigation of the core structure of suction vortices, from the formative stage (S~0.15) through intensification to the final demise (S~0.4) in undergoing transition to a 2-cell structure along the entire length. New experimental techniques have been devised in order to effectively address the shortcomings inherent in previous experimental work, particularly in the area of vortex wander. Radial profiles of velocity have been obtained using a hot film sensor passing through the vortex center, at various heights, for several swirl ratios and over

surfaces having different degrees of roughness. An analytical procedure has been developed to resolve the velocity data into its separate components, and which also enables other products, such as core radius and vertical vorticity to be determined.

2. EXPERIMENTAL TECHNIQUE
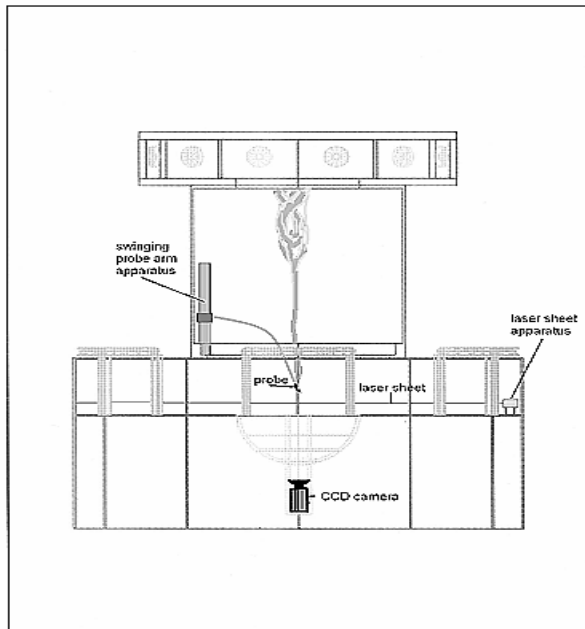
Figure 2. Schematic of Miami University TVC

Figure 2 illustrates the Miami University tornado vortex chamber (TVC) and much of the equipment required for data acquisition. The TVC has been substantially modified since an earlier description (Church and Snow, 1993), particularly in regard to its internal dimensions and to the manner in which the swirl is controlled. Circulation is introduced into the inflow via a set of short curved vanes. A vertical array of horizontal nozzles is located on the convex side of each vane. A particular swirl ratio is then obtained according to the flow rate through the nozzles. This feature is illustrated in Figure 3.

Velocity data were obtained via a single hot film sensor attached to a scanning arm. Descending at a 45° angle into the chamber's convergence region, the scanning arm is mounted on a rotating base, allowing the sensor to make periodic sweeps through the vortex core.
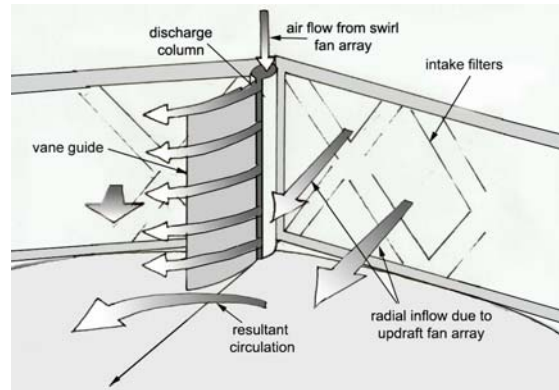
Figure 3. Schematic of swirl control system

Oriented perpendicular to the flow and scanning at a rate of 2000 samples/second, each sweep through the vortex core yielded a profile of total velocity. Apart from the surface layer the flow in the core is essentially helical, comprising vertical and tangential velocity components. The height of the scanning arm is continuously adjustable throughout a significant depth of the chamber; thus velocity measurements were repeated at several different heights through the supercritical core, ranging upwards from about 1 mm above the surface. Using photometric techniques, it was possible at all times to determine the location of the probe with respect to the vortex core. For the purpose of visualization a small amount of smoke was introduced into the vortex. Coincident with the height of the sensor, a diode laser illuminated a horizontal cross-section of the vortex. Images of this illuminated cross-section, taken from a CCD camera located beneath a small glass plate at the center of the chamber's floor, were displayed on a television monitor in real-time. These images were also recorded on Hi8 tape, allowing for the playback of sensor sweeps in slow motion. Therefore, only data corresponding to the successful passage of the sensor through the center of the vortex core were kept for analysis. The sensor data was visualized and processed using LabVIEW software, which allowed for data of interest to be archived for analysis. This procedure was repeated over for range of swirl ratios, comprising the intensity spectrum of supercritical vortices. The effects of surface roughness were examined by covering a portion of the chamber floor with a quasi-homogeneous rough surface.

For a more detailed description of the experimental technique see Kosiba (2002).

3. RESULTS FOR SMOOTH SURFACE

In this section we describe the data obtained over an aerodynamically smooth surface, a polished aluminum plate. Figure 4 shows an example of the velocity profile associated with a moderate swirl 1-cell and higher swirl 2-cell vortex. The 1-cell vortex exhibits a single sharp peak whereas the 2-cell type shows two velocity maximums with a turbulent central core.
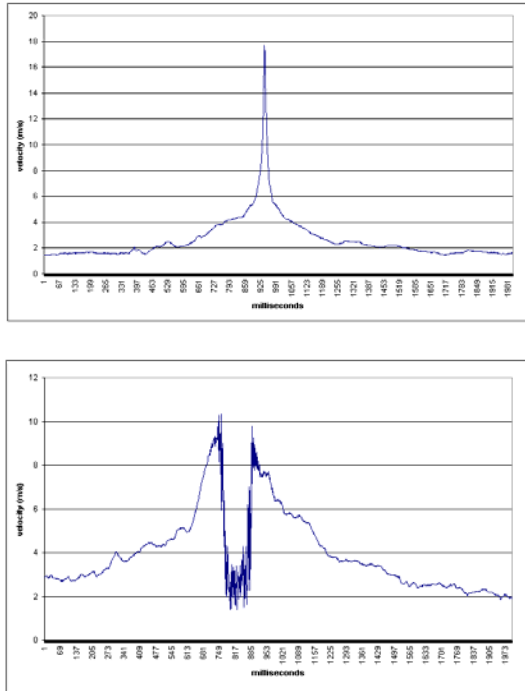
Figure 4. Total velocity data obtained from scan through 1-cell vortex (upper figure) and 2-cell vortex (lower figure)

Figure 5 shows two examples of the velocity profiles that were obtained at very low swirl (S~0.15), i.e. in the formative stage of the 1-cell vortex. These data, which verify visual observations, show that under steady background conditions the core flow alternated between a 1-cell form and a 2-cell-like form. Velocity profiles were obtained at the following swirl ratios: S=0.22, 0.29, 0.35, 0.37, 0.39, and at several heights from 2 mm above the surface to a maximum height that depended on the vertical extent of the 1-cell structure. For S=0.22 this amounted to practically the entire depth of the TVC, whereas for S=0.39 the average position of the VBD was about 1 cm above the surface, thus limiting the scanning levels to just 2 and 6 mm.
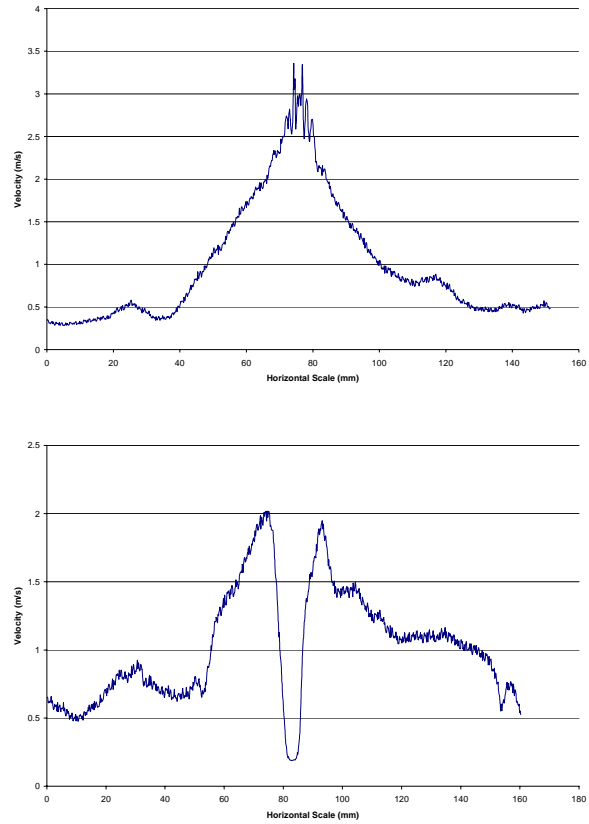
Figure 5. Examples of velocity profiles obtained under identical flow conditions during the formation stage of a suction vortex

Figures 6 and 7 show the on-axis (vertical) velocity maximum versus height for S=0.22 and S=0.39 respectively. The vertical scale has been non-dimensionalized with respect to the TVC inflow depth (280 mm), and the velocity with the mean updraft velocity in the TVC (0.56 msec^{-1}). (Note the difference in vertical scales in these two figures). In Figure 6 we see that the non-dimensional axial velocity rises to a maximum value of 8 at a non dimensional height of around 0.1, remaining fairly constant above that level. For the higher swirl case, in Figure 7, the maximum velocity is double that in Figure 6, and is achieved at a level that is only 1 or 2% of the inflow depth. This shows that high wind velocities are present much closer to the surface in the higher swirl vortices.
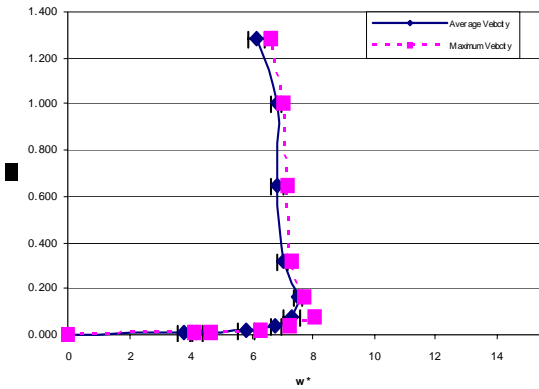
Figure 6. Axial Velocity versus height for S= 0.22
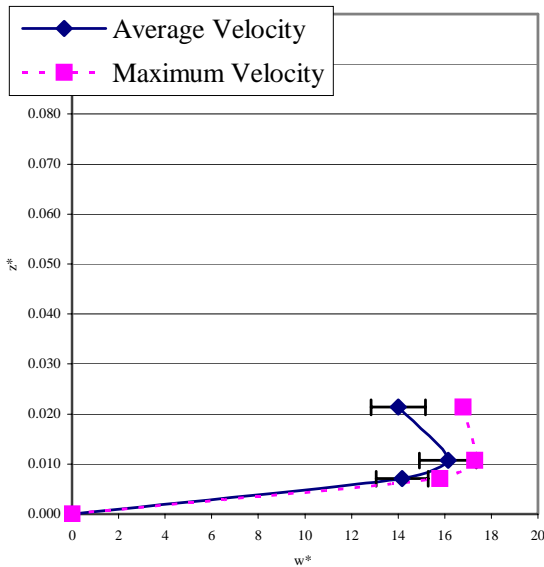
Figure 7. Axial velocity versus height for S = 0.39

It was observed that successive scans through the same vortex did not yield identical data, although the profiles bore a strong similarity, both in the profile width and the peak velocity. In order to obtain profiles that were characteristic of each height and swirl ratio, the data were subjected to an averaging process which also rendered the profiles symmetrical, as seen in Figures 8 and 9. These figures present dimensional velocity versus radial distance at selected heights: 2, 6 and 45 mm in Figure 8 (S=0.22), and only at 2 and 6 mm in Figure 9 (S=0.39). Both figures show the broadening of the profile with height, although it is more pronounced in the lower swirl case.
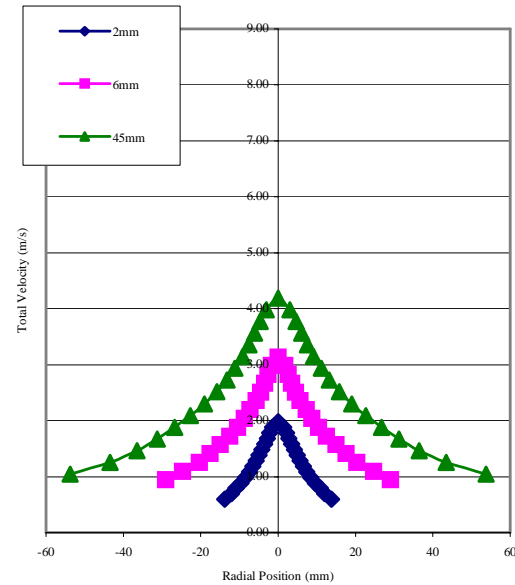
Figure 8. Radial profiles of total velocity for 3 heights, S = 0.22
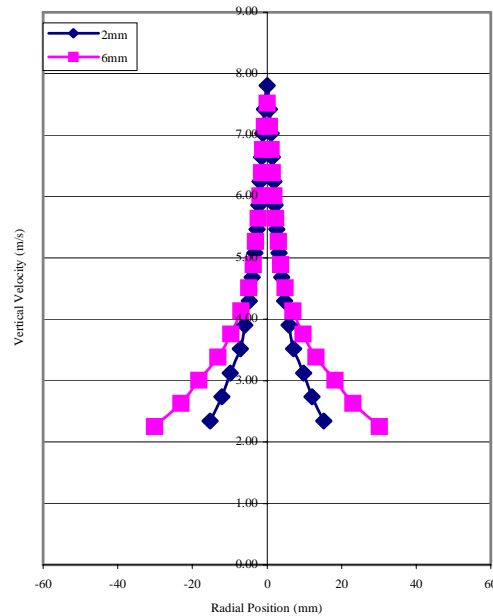
Figure 9. Radial profiles of total velocity for 2 heights, S = 0.39

The full width at half maximum (FWHM) was taken as the characteristic width of the velocity profile, and in Figure 10 the FWHMs at levels up to 90 mm are shown for 3 swirl ratios, S=0.22, 0.29 and 0.35. The higher swirl cases are

not included in this figure because of their limited vertical extent, but the trend is the same: these data confirm earlier visual observations that, as the degree of swirl increases, the vortex core shrinks
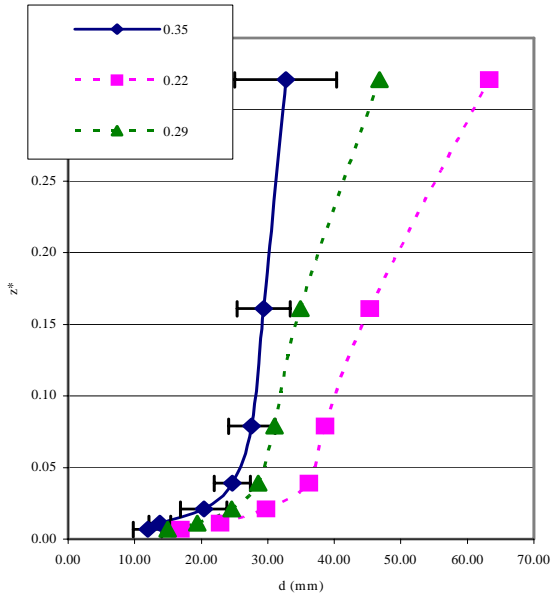
Figure 10. Profile width (FWHM) versus height for 3 swirl ratios

Although vortex wander had been greatly reduced it was still present. The vortex became more unsteady as the degree of swirl increases, as exemplified by more rapid lateral displacements and vertical oscillations of higher frequency in the VBD region. At the higher swirls the peak values of velocity showed greater variability than the profile width.
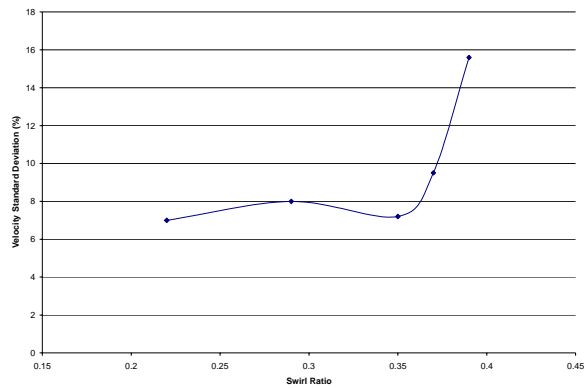
Figure 11. Standard deviation in peak velocity as a function of swirl ratio

Figure 11 shows, for the 6 mm level, how the standard deviation of the peak velocity increases as the swirl ratio increases. The more variable nature of higher swirl vortices has implications for their impact on surface structures.

4. ROUGH SURFACE DATA

Similar procedures were adopted for rough surfaces as for the smooth surface, although the measurements were less comprehensive. Three different degrees of surface roughness were implemented, in ascending order of roughness as follows: a layer of coarse (24 grit) sandpaper, designated RS1, a checkerboard pattern mat consisting of alternating 6 mm squares and spaces (RS2), and an artificial turf having length elements of about 1 cm (RS3). For each case a small (5 cm diameter) viewing window was placed at the center, and the rough materials perforated accordingly to allow smoke to penetrate for visualization purposes. The overall effect of surface roughness as it affects the most general characteristics of the velocity profile, namely the peak axial velocity and the FWHM, is shown in Figures 12 and 13. These data were obtained at a height of 45 mm. Figure 12 compares of the peak vertical velocities for vortices over rough surfaces with those over the smooth surface. For RS1 and RS2 there is a clear trend, that roughening the surface decreases flow velocities to an extent that depends on the degree of roughness. However the trend is not reflected in the RS3 data, where peak velocities are higher than one or both of the other two rough surfaces and in a way that depends on the degree of swirl.
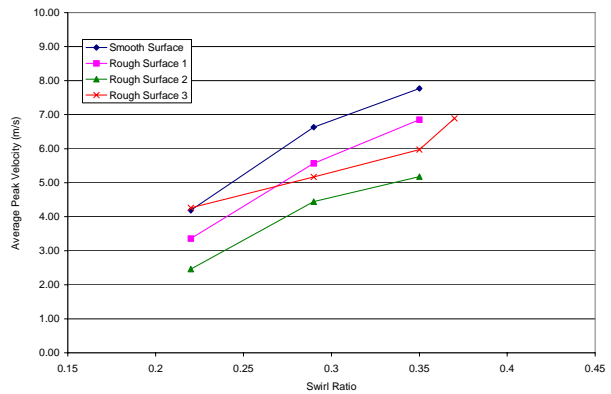
Figure 12. Comparison of peak velocities for all surfaces, smooth and rough

Figure 13 presents the corresponding FWHM data, and similar trends are seen in the profile width: for RS1 and RS2 the effect of surface roughness was to broaden the profile, but not so for RS3, the roughest surface. We conclude that, by reducing peak velocities and broadening the profile, a moderate degree of roughness (RS1/RS2) has the effect of producing a vortex flow that is similar to what would be obtained over a smooth surface but at a lower swirl. A very rough surface, on the other hand, seems to affect the structure of the core flow in a more radical way, made more complex in that it also seems to depend upon the degree of swirl. In particular, at low swirl the peak velocities are comparable with the smooth surface and the profile is narrower; at higher swirl the widths are comparable with the smooth surface and the velocities are smaller.
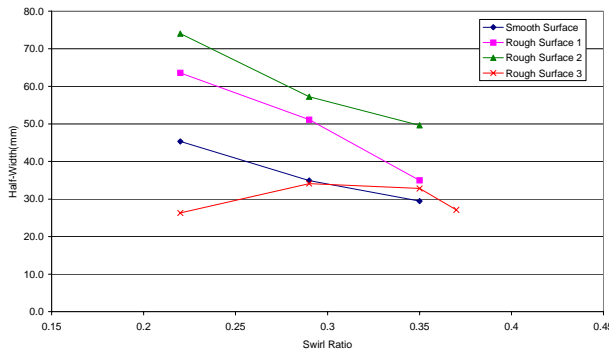
Figure 13. Comparison of FWHM data for all surfaces, rough and smooth

5. ANALYSIS OF PROFILES

As shown above, the average velocity profiles, in spite of different peak values and widths seem similar in shape. In order to examine this similarity more closely, the profiles were normalized and overlaid. Figure 14 shows the normalized profiles for S=0.35, for six different sampling heights, ranging from 3 mm to 90 mm. Inspection of this figure shows a high degree of similarity in profile shape for these levels. (At levels that were well above the surface this was found to not be the case, as there the peaks tended to flatten out).
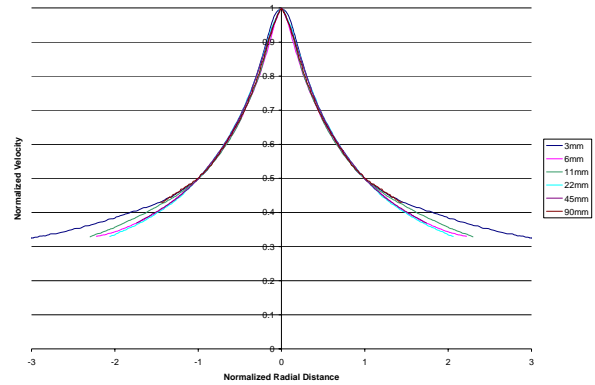
Figure 14. Superposition of normalized total velocity profiles, various heights, $S = 0.35$

In Figure 15 we compare the normalized profile shape for three different swirl ratios at the 45 mm level. Again, a very close resemblance is demonstrated. We conclude from these and other results that, with regard to the shape of the total velocity profile of 1-cell tornado-like vortices, any dependence on either swirl ratio or height is slight. Bear in mind that this conclusion is based on the averaged profiles and, as stated earlier, successive scans through the same core region show some degree of variability.
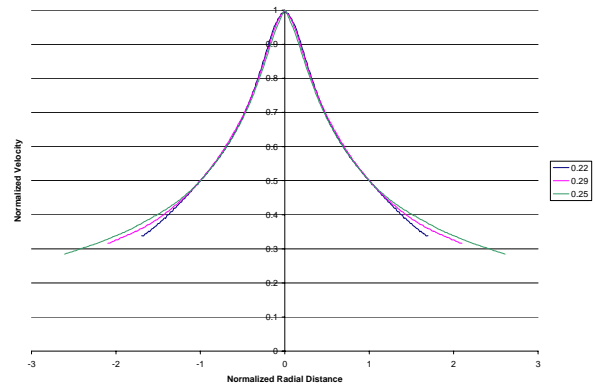
Figure 15. Superposition of normalized total velocity profiles, various swirl ratios, 45mm height

A single velocity sensor, such as was used here, lacks the inherent capacity to resolve the data into the respective components, in this work these being the vertical and tangential components. However, we can make educated guesses about the component values in the vicinity of the axis, and consequently develop an approximate representation of the radial distribution of each component. For example, we

expect the vertical velocity component to assume a Lorentzian form close to the axis, and we note also that other functional forms (e.g. Gaussian, jet-like) all devolve to the same shape at small radius. A linear increase of tangential velocity close to the axis was assumed. Baker (1981) developed a scheme in which, for one particular vortex, he was able to determine each velocity component separately. In a close examination of Baker's data we found that a Lorentzian profile fitted the vertical velocity not only close to the axis but at larger radius as well. From the near axis data a radial scaling value was derived for each profile, from which the vertical velocity profile was produced. The tangential velocity profile was obtained by vector subtraction of the vertical velocity profile from the total velocity data.

A sample result is shown in Figure 16. The radial distributions of vertical and tangential velocities are shown dimensionally for a vortex (S=0.35) over a smooth surface and at height of 45mm. This shows the vertical velocity decreasing from an on-axis value of 7.8 msec^{-1} and the tangential velocity increasing to a maximum value of 5.4 msec^{-1} at a radius of 5 mm. The tangential velocity profile is rather flat near the peak, being within 90% of the peak value from a radius of 3 mm to 9 mm. We note that here the ratio of maximum tangential to maximum vertical velocity is 0.69, and have found that generally the ratio for other cases falls between 0.6 and 0.7. To date most of the analysis has been applied to the smooth surface data, and because of a greater variety in the shapes of profiles over rough surfaces, much of the rough surface data may not be suited to this analytical process. However in Figure 17 we are showing the same quantities, for the same swirl ratio and height as in Figure 16, the only difference being that this is for a vortex formed over the least rough surface (RS1). At first sight Figures 16 and 17 look quite similar, but there are noticeable differences, namely that over the rough surface the peak values of both components have been reduced by several percent and the radius of maximum tangential velocity has also increased. These results are in accord with expectations.
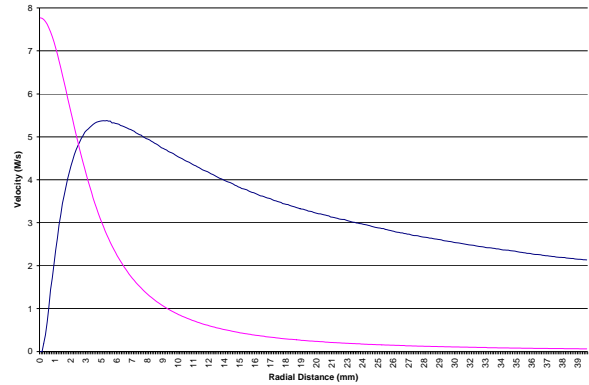
Figure 16. Vertical and tangential components for smooth surface, S = 0.35
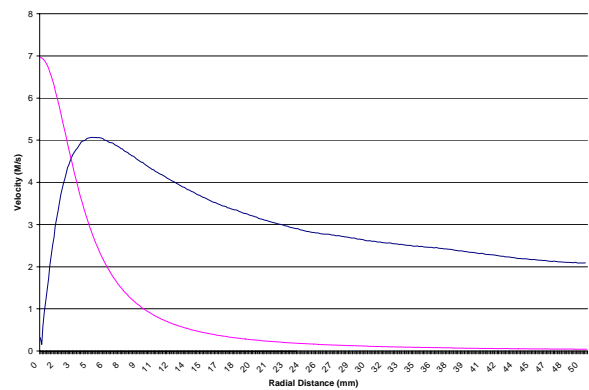
Figure 17. Vertical and tangential components for rough (RS1) surface, S = 0.35

Figure 10 showed profile width (FWHM) versus height as a function of swirl ratio. Figure 18 now shows vortex core radius (i.e. radius of maximum tangential velocity) versus height as a function of swirl ratio. The results show that the core radius increases with height, more rapidly with height close to the surface and less rapidly at higher levels. As with Figure 10, we see that the core radius decreases as the swirl ratio increases.
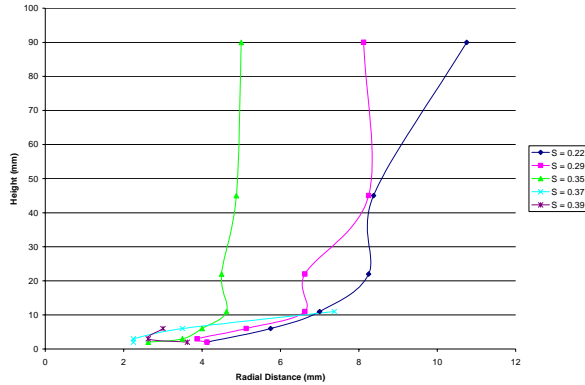
Figure 18. Derived values of core radius versus height, various swirl ratios

From the tangential velocity data shown in Figure 16, the vertical vorticity can be derived at each radial position. In figure 19 the radial distributions of vorticity are shown for several heights ranging from 3 mm to 90 mm. The highest vorticity values are seen to be located well within the core region, close to the axis.

In the highest swirl cases (S=0.37, S=0.39) the peak vorticity values were close to $10^4 sec^{-1}$.
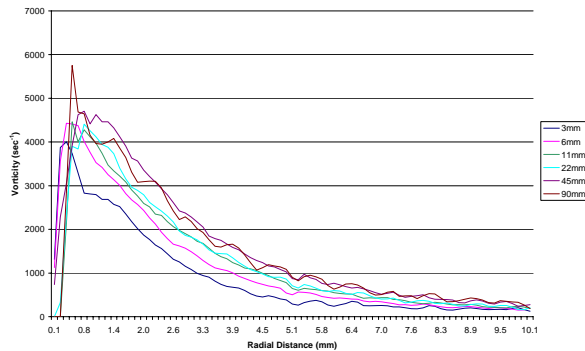
Figure 19. Vertical vorticity versus radius at several heights, S = 0.35

6. SUMMARY AND CONCLUSIONS

Suction vortices represent the most intense manifestation of tornadic winds in that they are capable of placing the strongest winds closest to the surface, and to a greater degree than any other atmospheric phenomenon. This research has focused on a study of suction vortices in the laboratory in order to provide data that illustrate a number of related aspects, namely: the processes which accompany the formation of suction vortices, the parameters that affect their intensity, the magnitudes of attainable velocities, and core size and structure. Although much has been inferred in the past from visual observations of vortex phenomena, a purpose here was to provide a quantitative basis for the conclusions. Although several investigators in the past have made detailed measurements on one or two specific cases, the intention here has been to consider suction vortices over the complete range of intensities. As stated earlier, using swirl ratio as an indicator of vortex intensity and structure, suction vortices exist at the surface over a range of swirl ratios from ~0.15 to~0.4, and they have the strongest winds at the upper end of this range, other factors being constant. For this research we developed a tornado vortex chamber whose interior dimensions are similar to those used in earlier laboratory studies (e.g. Ward, 1972; Church et al, 1979). The problem of vortex wander was addressed and to a large extent overcome, thus making in situ measurements more practicable. A scanning sensor system was developed which, in conjunction with video hardware and data acquisition software, enabled efficient, reliable data collection. Principal conclusions are discussed below.

During the low swirl (S~0.15) formative stage of the vortex two distinct velocity profiles emerged (Figure 5). The single peak profile was associated with the development of a concentrated core at the surface and fed by a low level radial inflow which penetrated close to the axis. The concentrated core appeared sporadically, to be soon replaced by a core more diffuse in appearance. The second profile, showing a stagnant center was associated with the diffuse core. In this case the low level radial inflow appeared to separate before getting close to the axis. Transition back to the concentrated core was accompanied by a bubble of fluid from the surface being transported downstream in the vortex. We infer that these two forms are related to the radial pressure gradient near the surface, which is considered to switch back and forth between a favorable and an adverse pressure gradient: with a favorable pressure gradient a concentrated core exists, with an adverse pressure gradient the flow separates and gives rise to low velocities at the center of the core.

Scanning through the same vortex yielded slightly different velocity profiles on each scan, some peaks being more rounded, others more cusp-like. The on-axis vertical velocity increased rapidly with height near the surface to a maximum at some level, above which its magnitude remained relatively constant. The maximum velocity is typically one order of magnitude greater than that of the updraft in which they form, and in the limiting case where the vortex breakdown region is close to the surface the maximum velocity approaches 20 times the mean updraft velocity. At higher swirl ratios the position of the maximum vertical velocity was closer to the surface. The region in which the vertical velocity increases with height is one of convergence, in which the core flow is supplied by a low level radial inflow. As the swirl ratio increases the core flow is supplied by a progressively thinner inflow layer in which there are correspondingly higher radial velocities. Thus the overall effect of increasing the swirl is to place ever higher velocities closer to the surface. Another factor which is also swirl ratio dependent is the degree of unsteadiness in the flow, as demonstrated in Figure 11. In the natural environment this flow property, which is particularly pronounced at high swirl, produces violent impulses that can contribute significantly to the damage. Thus we see damage as being created as a consequence not only of steady wind forces but also because of the fluctuating nature of winds at a point.

The full widths at half maximum were determined for the total velocity profiles, and used as a means of assessing the factors that affected "core size". Thus it was seen that core size increased rapidly with height close to the surface and more gradually at higher levels. The core size decreased as the degree of swirl in the background flow increased, confirming earlier visual observations (Church et al, 1979). A procedure was developed by which the total velocity data was resolved into separate velocity components. This was based on an assumed profile shape (Lorentzian) for the vertical velocity, a shape that is consistent with Baker's (1981) data. By this means radial distributions of tangential and vertical velocity, and consequently other products such as core radius and vertical vorticity, were derived. The procedure was repeated using other functional forms for the vertical velocity (Gaussian, jet-like), and these produced results which differ by a few percent in products such as maximum velocities and core radii. As an example, the ratio of maximum tangential velocity to maximum vertical velocity was found to be in the range 0.6-0.7 for any of the functional forms used. We conclude that the procedure provides a fair representation of vortex core structures, although it does not obviate the need for more sophisticated sensing techniques using multiple sensors.

For a given swirl ratio roughening the surface resulted in an increased core size and also reduced maximum velocities. These results point to surface roughness as having the effect of causing a vortex to have the same structure as one at a lower swirl ratio over a smooth surface. This agrees with the Leslie's (1977) conclusions. Earlier Dessens (1972) had reported an increase in maximum velocity associated with increased surface roughness. However from an examination of Dessens' data it now becomes clear that in his experiment the vortex that formed over the smooth surface was a 2-cell vortex, and it would be entirely consistent that roughening the surface would cause transition to a lower swirl, higher velocity 1-cell flow. As in Rostek's (1985) results, it was found that a highly roughened surface affected the vortex anomalously. Although efforts are continuing to provide a satisfactory interpretation of the data for the roughest surface, one may also question the significance of this particular feature in relation to tornadoes and their interaction with the physical environment.

7. REFERENCES

Baker, G. L., 1981: Boundary layers in laminar vortex flows, Ph.D. thesis, Purdue University, West Lafayette, Indiana.

Church, C. R., J. T. Snow, G. L. Baker and E. M. Agee, 1979: Characteristics of tornado-like vortices as a function of swirl ratio: a laboratory investigation. *J. Atmos. Sci.*, 36, 1755-1776.

Church C. R. and J. T. Snow, 1993: Laboratory models of tornadoes. *The Tornado: Its Structure, Dynamics, Prediction and Hazards*, C. R. Church et al., Eds., Amer. Geo physical Union, pp. 277-296.

Davies-Jones R. P.,1976: Laboratory simulations of tornadoes. *Proceedings, Symposium on Tornadoes, Assessment of Knowledge and Implications for Man*, R. E. Peterson, Ed., Texas Tech University, Lubbock, Texas, pp. 151-174.

Dessens, J., 1972: Influence of ground surface roughness on tornadoes: a laboratory simulation. *J. Applied Meteorology*, 11, 72-75.

Kosiba, K. A., 2002: A laboratory investigation of the velocities in and the effects of surface roughness on tornado-like vortices, M. S. thesis, Miami University, Oxford, Ohio.

Leslie, F. W., 1977: Surface roughness effects on suction vortex formation: a laboratory simulation. *J. Atmos. Sc*i., 34, 1022-1027.

Rostek, W. F.,1985: Surface roughness effects on tornado-like vortices, M. S. thesis, Purdue University, West Lafayette, Indiana.